Macromolecules

Article

pubs.acs.org/Macromolecules

Formation of Hyperbranched Amphiphilic Terpolymers and Unimolecular Micelles in One-Pot Copolymerization

Xu Wang,*[,†] Lianwei Li,[†] Weidong He,[‡] and Chi Wu*[,†,§]

[†]Hefei National Laboratory for Physical Sciences at the Microscale, Department of Chemical Physics, and [‡]CAS Key Laboratory of Soft Matter Chemistry, Department of Polymer Science and Engineering, University of Science and Technology of China, Hefei, Anhui 230026, China

[§]Department of Chemistry, The Chinese University of Hong Kong, Shatin, N.T., Hong Kong

ABSTRACT: Utilizing self-assembled structures made of small molecular surfactants or linear amphiphilic copolymers to encapsulate hydrophobic chemicals generally faces a dilution challenge due to their critical micelle concentrations. In this study, we designed a one-pot self-condensing vinyl terpolymerization of poly(ethylene glycol) methyl ether methacrylate (PEG) and methacrylic acid (MAA) in *n*-butyl acetate by using a vinyl-functionalized chain transfer agent (C_{12}-raft). In the presence of hydrophobic epoxiconazole (EP) as a model chemical that can complex with MAA, the resultant amphiphilic hyperbranched terpolymer chains can form unimolecular micelles with EP encapsulated inside. The effects of monomer composition and EP content on the stability of the resultant dispersions in both *n*-butyl acetate and redispersing water were studied by combining static and dynamic laser light scattering, transmission electron microscopy, and ultraviolet−visible spectroscopy. We found the optimal encapsulation and stabilization molar ratio of [MAA]:[EP] = 1.0:0.8. Under such optimal conditions, the resultant dispersions can be stabilized for months in *n*-butyl acetate, good for storage, and for hours after redispersion in a large amount of water, sufficiently long for the field applications. Note that the principle demonstrated here is readily applicable to the dispersion and stabilization of other hydrophobic active ingredients, not only agrochemicals but also drugs, with some properly chosen monomers.

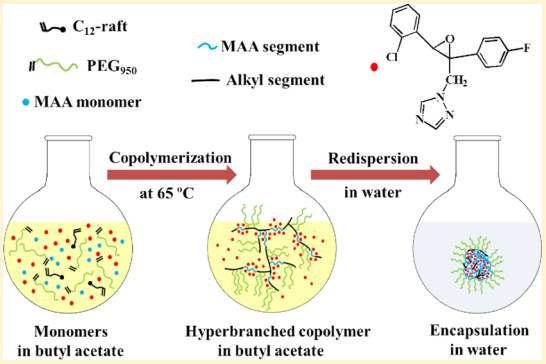

INTRODUCTION

These years, various strategies for dispersing hydrophobic chemicals have been developed, including solid dispersions,[1−3] cyclodextrin inclusion complexes,[4−7] emulsions and microemulsions,[8−11] and nanosuspensions.[12,13] Recently, polymeric micelles made of the self-assembly of amphiphilic copolymers consisting of hydrophobic and hydrophilic segments have been extensively developed as drug and chemical carriers,[14−22] some of which are responsible to their surrounding environmental changes.[23] In most of the cases, the copolymers are synthesized and mixed with active chemicals under a certain condition to encapsulate them inside the hydrophobic core via the hydrophobic or specific interaction, while the hydrophilic blocks form a shell to stabilize the micelle-like structure. The cost and the loading efficiency are usually problems in such formulations, which might be workable for biomedical applications but certainly not practical for agricultural applications in which a cheap formulation and a typical loading of 20−40% w/w of active chemicals are often required.

Practically, concentrated dispersions or suspensions of active agrochemicals, including fungicides, pesticides, insecticides, nematicides, and herbicides, are often formulated, shipped, and sold to reduce the transportation cost. Such concentrated dispersions or suspensions have to be redispersed (diluted) in a large amount of water (50−100 times or more) before their field applications. Because of the existence of the critical micelle or aggregation concentration (CMC or CAC), the dilution could lead to easy aggregation and/or crystallization, especially when linear di- or tri-block copolymers are used,[23] lowering the bioavailability. Therefore, any formulation faces three unavoidable and difficult problems: (1) only using commercially available chemicals/monomers to make the formulation economically viable, (2) loading the active hydrophobic ingredient as much as possible to form a concentrated dispersion or suspension which is stable for at least 18 months, and (3) maintaining the stability of the redispersion of such a formed concentrated dispersion or suspension in a large amount of water for a sufficiently long time (few hours) before their field applications.

To solve such a dilution problem, hyperbranched and dendritic-like amphiphilic copolymers were designed and developed as drug and active ingredient carriers because they could form unimolecular micelles with many functional ends to interact with active chemicals to increase the loading efficiency.[16,24−30] In the current study, we moved further by designing self-condensing vinyl polymerization (SCVP) of

Received: July 22, 2015
Revised: September 11, 2015
Published: September 24, 2015

DOI: 10.1021/acs.macromol.5b01637
Macromolecules 2015, 48, 7327−7334

commercially available monomers of methacrylic acid (MAA), poly(ethylene glycol) methyl ether methacrylate (M_n = 9.5 × 10^2 g/mol, PEG_{950}), and a vinyl-functionalized chain transfer agent (C_{12}-raft) through reversible addition−fragmentation transfer polymerization (RAFT) in *n*-butyl acetate, in which MAA can complex with a model chemical, epoxiconazole (EP), as shown in Scheme 1.

Scheme 1. Schematic of Formation of Amphiphilic Hyperbranched Poly(MAA-*co*-C_{12}-*g*-PEG_{950}) Terpolymer and Its Complexation with EP in *n*-Butyl Acetate via Self-Condensing Vinyl Polymerization (SCVP) and Its Redispersion in Water

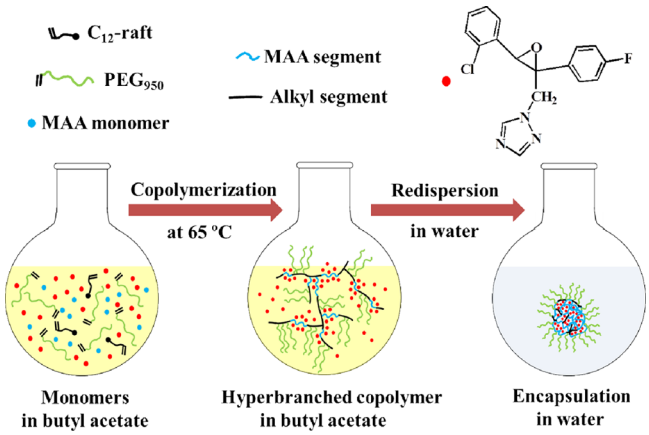

EP is a fungicide active ingredient to inhibit the ergosterol biosynthesis and disrupt the formation of fungal cell membrane.[31,32] Its low solubility in water (~6.6 mg/L at 20 °C) limits its field application and bioavailability.[32] Current technology is to mill it into small particles and then suspend them in water with stabilizers. In our design, MAA, PEG_{950}, C_{12}-raft, and EP are all soluble in *n*-butyl acetate; MAA can complex with EP via hydrogen bonds; and C_{12}-raft has a trithiocarbonate group and a methacrylate group, respectively, at its two ends, acting as a chain transfer agent and also a comonomer so that it builds up a hyperbranched skeleton. In the resultant EP/terpolymer complexes, EP/poly(MAA-*co*-C_{12}-*g*-PEG_{950}), the hyperbranched chain backbone made of poly(MAA-*co*-C_{12}) complexed with EP becomes insoluble in *n*-butyl acetate, but the grafted PEG_{950} chains stay on its periphery to stabilize the unimolecular micelle-like structure and prevent interchain association. In such a novel design, the copolymerization encapsulates and stabilizes EP in one step. The principle demonstrated here can be readily used for other active ingredients with a proper choice of comonomers.

Note that the introduction of hydrophobic C_{12} segments and the complexation between MAA and hydrophobic EP further stabilize the insoluble hyperbranched chain backbone by an unconventional viscoelastic effect.[33,34] Namely, when two insoluble chains approach each other, the interchain association involves two characteristic time scales: the chain relaxation time (τ_R) that allows two chains to relax, penetrate, and intertwine with each other and the chain contact (interaction) time (τ_C). If $\tau_R \gg \tau_C$, two approaching chains behave like two tiny glass balls so that they are bouncing away, and the collision leads to no larger interchain aggregates. In our design, grafting hydrophilic PEG on the periphery of each hyperbranched chain reduces τ_C, and incorporating hydrophobic C_{12} segments, and the complexation between MAA and hydrophobic EP increase τ_R at the same time. Therefore, each hyperbranched chain is kinetically stabilized when $\tau_R \gg \tau_C$. As expected, there is no critical micelle concentration (CMC) problem in the dilution of such unimolecular micelle dispersion into a large amount of water. The dilution would result in a core−shell micelle-like structure with a hydrophobic core made of the collapsed hyperbranched chain backbone with complexed EP and a hydrophilic shell comprising the extended PEG chains.

In current work, we demonstrated a novel principle of how to form and use amphiphilic hyperbranched copolymer chains to stabilize hydrophobic active chemicals and reach two objectives: forming a stable dispersion in its reaction medium via a one-step copolymerization and playing the viscoelasticity to form a stable redispersion in a large amount of water for its field application. The principle demonstrated here is readily applicable to encapsulate other active chemicals for various applications because we have overcome the dilution problem.

EXPERIMENTAL SECTION

Materials. Methacrylic acid (MAA, Sinopharm, AR) and *N*,*N*-dimethylformamide (DMF, Sinopharm, AR) were distilled under a reduced pressure over $MgSO_4$ prior to use. Poly(ethylene glycol) methyl ether methacrylate (PEG_{950}, M_n = 9.5 × 10^2 g/mol, Sigma-Aldrich) was passed through a basic alumina column to remove the inhibitor. *n*-Butyl acetate (Sinopharm, AR) was stirred over CaH_2 overnight and distilled under a reduced pressure before use. Epoxiconazole (EP, BASF Corporation) was recrystallized twice from ethanol and dried in oven overnight. Azobis(isobutyronitrile) (AIBN, Aldrich, 99%) was recrystallized twice from methanol. Milli-Q water with a resistivity of 18.2 MΩ·cm was used. Other reagents were used as received without further purification unless noted otherwise.

Synthesis of Chain Transfer Agent C_{12}-raft (III). In Scheme 2, *S*-1-dodecyl-*S*′-(*R*,*R*′-dimethyl-*R*″-acetic acid) trithiocarbonate (**I**) was synthesized using a procedure detailed before.[35] 2-Hydroxyethyl methacrylate (**II**) was used after the removal of the inhibitor. 20.0 g of **I** (54.9 mmol), 8.6 g of **II** (66.1 mmol), and 0.68 g of 4-(dimethylamino)pyridine (DMAP) (5.6 mmol) were dissolved in 100.0 mL of CH_2Cl_2. After stirring at room temperature for 10 min, 12.6 g of 1-(3-dimethylaminopropyl)-3-ethylcarbodiimide hydrochloride (EDC) (65.9 mmol) dissolved in 50.0 mL of CH_2Cl_2 was added dropwise into the solution within 30 min under N_2 flow. The mixture was further added 100.0 mL of CH_2Cl_2 and stirred overnight at room temperature. After the reaction, CH_2Cl_2 was partly removed by evaporation. The remaining solution was washed three times with saturated NaCl aqueous solution. The organic phase was dried with anhydrous $MgSO_4$. After removing the solvent, the product was purified by column chromatography over silica gel eluting with hexane/ethyl acetate (5:1, v/v). The final product (**III**, yellow oil) was obtained after the removal of hexane and ethyl acetate.

Synthesis of Hyperbranched Amphiphilic Copolymer Chains with Encapsulated EP. Different conditions of copolymerization of

Scheme 2. Schematic of Synthesis of Chain Transfer Agent C_{12}-raft (III)

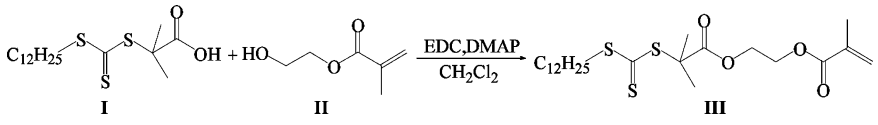

DOI: 10.1021/acs.macromol.5b01637
Macromolecules 2015, 48, 7327−7334

MAA, PEG_{950}, and C_{12}-raft with and without EP were used. In a typical reaction (EP-0.6), a reaction flask equipped with a magnetic stirrer and a rubber septum was charged with 0.261 g of MAA (3.03 mmol), 1.50 g of PEG_{950} (1.58 mmol), 0.010 g of C_{12}-raft (0.0209 mmol), 0.60 g of EP (1.82 mmol), 2.5 mg of AIBN (0.0152 mmol), and 10.0 mL of *n*-butyl acetate. The flask was degassed by three freeze−pump−thaw cycles, backfilled with N_2, and placed in an oil bath at 65 °C to start the copolymerization for 15 h to form a hyperbranched terpolymer denoted as poly(MAA-*co*-C_{12}-*g*-PEG_{950}).

Characterization. ^{13}C nuclear magnetic resonance (NMR) spectra were recorded on a Bruker AV400 spectrometer using deuterated toluene (toluene-d_8) as solvent. The transmission electron microscopy (TEM) images were obtained using an FEI CM120 microscope operated at 120 kV. The preparation of the TEM samples is outlined as follow. The dispersion was first filtrated by a 0.45 μm PTFE filter after a dilution of EP-0.6 in *n*-butyl acetate with a final concentration of ~0.25 g/L. The sample grid was placed on the bottom of a small cell, a tiny drop of the dispersion (~20 μL) was added on the grid, and the dispersion was frozen when the cell was immersed into liquid nitrogen; the solvent was removed by freeze-drying under high vacuum before the TEM measurements. The ultraviolet−visible (UV−vis) measurements were done using a UNICO 2802PCS UV/vis spectrometer in the wavelength range 200−400 nm. The transmittance of the solution was measured in a quartz cuvette.

Laser Light Scattering (LLS). A commercial LLS spectrometer (ALV/DLS/SLS-5022F) equipped with a multidigital time correlator (ALV5000) and a cylindrical 22 mW He−Ne laser (λ_0 = 632.8 nm, UNIPHASE) as the light source was employed for dynamic and static LLS measurements. The details of LLS instrumentation and theory can be found elsewhere.[36,37] In static LLS,[38] the angular dependence of the absolute excess time-average scattering intensity, the Rayleigh ratio $R_{vv}(q)$, can lead to the weight-average molar mass (M_w), the root-mean-square gyration radius $\langle R_g \rangle$, and the second virial coefficient A_2 by

$$\frac{KC}{R_{vv}(q)} \approx \frac{1}{M_w}\left(1 + \frac{1}{3}\langle R_g^2\rangle_z q^2\right) + 2A_2C \quad (1)$$

where K is a constant and $q = (4\pi n/\lambda_0)\sin(\theta/2)$ with n and λ_0 being the solvent refractive index and the wavelength of light in vacuum. The dn/dC values of each of the resultant dispersions in *n*-butyl acetate and in DMF at 25 °C were determined by a precise differential refractometer.[39] For example, dn/dC of hyperbranched copolymer (EP-0.6) was 0.106 mL/g in *n*-butyl acetate and 0.053 mL/g in DMF at 25 °C.

In dynamic LLS,[37] the intensity−intensity time correlation function $g^{(2)}(t,q)$ in the self-beating mode was measured, where t is the decay time. Using a Laplace inversion, $G(\tau)$ can be calculated from the measured $g^{(2)}(t,q)$ and then inverted to a line-width distribution $G(\Gamma)$. For a pure diffusive relaxation, Γ is related to the translational diffusion coefficient D by $(\Gamma/q^2)_{q\to 0,C\to 0} = D$, so that $G(\Gamma)$ can be converted to translational diffusion coefficient distribution $G(D)$ and further converted to hydrodynamic radius distribution $f(R_h)$ via the Stokes−Einstein equation, $R_h = k_BT/6\pi\eta D$, with k_B, T, and η being the Boltzmann constant, the absolute temperature, and the solvent viscosity.

LLS characterizations of the hyperbranched copolymers with and without EP directly in *n*-butyl acetate and redissolved in a good solvent DMF lead to their apparent and absolute weight-average molar masses, respectively. For the copolymer without EP, the copolymer was twice precipitated into an excess amount of cold ether and dried before dissolved in its good solvent DMF. As expected, the LLS characterization leads to the weight-average molar mass of individual hyperbranched copolymer chains. For copolymers with EP, *n*-butyl acetate was removed by evaporation under a reduced pressure at 50 °C, and then the copolymer was dissolved in DMF with different concentrations before the LLS characterization. Note that soluble small EP molecules contribute very little to the intensity of the scattered light. The redispersion in water was typically done by adding a dispersion of the copolymer with or without EP in *n*-butyl acetate dropwise into pure water under stirring to reach a final volume ratio of *n*-butyl acetate:water = 1:50. Further application of 10 s ultrasonic irradiation in an ice bath disperses *n*-butyl acetate well into water to form a stable emulsion. Before the characterization, it was further diluted 10 times by water to form a clear aqueous solution.

RESULTS AND DISCUSSION

The solubility of EP in *n*-butyl acetate at 25 °C was measured to be ~8.2 × 10^{-2} g/mL, while significant enhancement of solubility was observed when a small amount of MAA (5.4 × 10^{-2} g/mL) was added. To confirm the origin of this enhancement, ^{13}C NMR spectra were carried out to study the interaction between MAA and EP molecules. Figure 1 shows a comparison of ^{13}C NMR spectra of MAA monomer and a mixture of MAA and EP in toluene-d_8. The shifts of peaks (a−c) to peaks (a'−c') clearly reveal the interaction between EP and MAA, presumably due to the hydrogen-bonding-induced complexation. Therefore, both the free and the complexed EP molecules exist in *n*-butyl acetate solution. Quantitatively, the molar ratio between MAA and EP was found to be ~3, which means three MAA molecules, on average, are able to complex with one EP molecule. This is reasonable because each EP molecule contains three potential nitrogen atoms for hydrogen bonding interaction. The rest of EP is dissolved in *n*-butyl acetate and exists as free molecules, but they are further encapsulated by the terpolymer chains via the hydrophobic interaction when the dispersion is diluted by water. In other words, the encapsulation of hydrophobic EP inside the copolymer in water is a result of a combination of hydrogen-bonding and hydrophobic interactions.

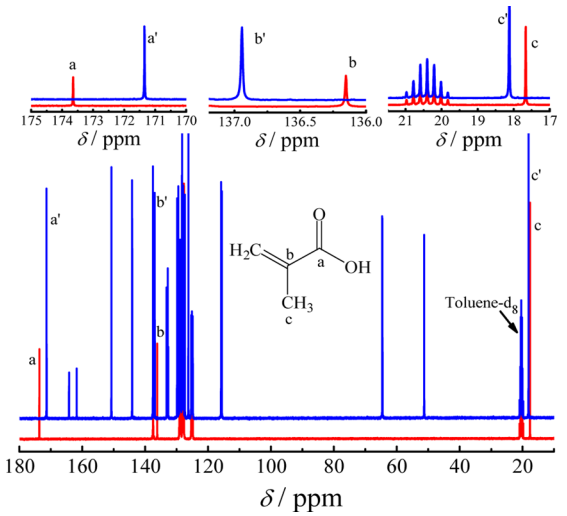

Figure 1. ^{13}C NMR spectra of MAA monomer (red line) and a mixture of MAA and EP (blue line) in toluene-d_8 at room temperature.

The copolymerization of MAA, PEG_{950}, and C_{12}-raft with and without EP in *n*-butyl acetate is a multidimensional problem and can result in clear solutions, emulsions, or suspensions, depending on the initial conditions. In principle, *n*-butyl acetate is a poor solvent for PMAA but a good one for PEG_{950}. Therefore, the comonomer composition and EP content affect the balance of the solvophilic and solvophobic components. We first studied the EP content effect on the appearance and stability of the resultant dispersions with a fixed amount of MAA (3.03 × 10^{-1} M), C_{12}-raft (2.09 × 10^{-3} M), and PEG_{950} (1.58 × 10^{-1} M), where "M" stands for "mol/L".

DOI: 10.1021/acs.macromol.5b01637
Macromolecules 2015, 48, 7327−7334

Table 1. Effect of EP Content on Appearance, Stability, and Characteristics of Resultant Dispersions Formed in One-Step Copolymerization of MAA (3.03×10^{-1} M), PEG_{950} (1.58×10^{-1} M), and C_{12}-raft (2.09×10^{-3} M) in *n*-Butyl Acetate

sample	[EP]/[MAA]	appearance	stability	$M_{w,app}$ (g/mol)	$\langle R_h \rangle$ (nm)	$\langle R_g \rangle$ (nm)	$\langle N_{agg} \rangle$
EP-0.0	0.0	slight milky	stable	1.35×10^6	17.0	19.7	1.4
EP-0.6	0.6	clear	stable	3.18×10^5	11.0	13.7	0.7
EP-0.8	0.8	clear	stable	2.38×10^5	11.0	13.2	0.7
EP-1.0	1.0	clear	unstable	1.82×10^5	11.0	15.5	0.9

The experimental conditions are summarized in Table 1. As shown in Figure 2, no visible precipitation or crystallization of EP in the resultant dispersions was observed shortly after copolymerization.

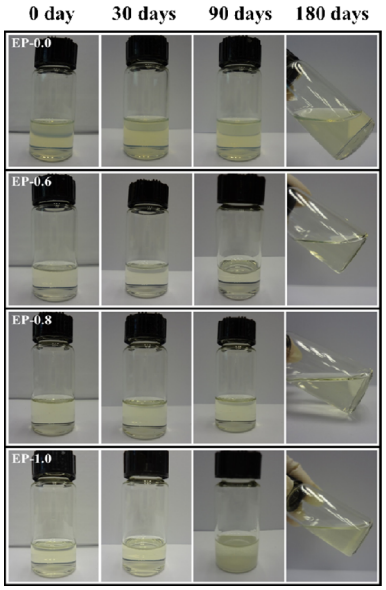

Figure 2. Photographs of time-dependent appearance and stability of different dispersions at room temperature after copolymerization.

In order to characterize individual poly(MAA-*co*-C_{12}-*g*-PEG_{950}) chains, we first dissolved each terpolymer in a good solvent DMF. Figure 3 shows a typical Zimm plot of poly(MAA-*co*-C_{12}-*g*-PEG_{950}) terpolymer (EP-0.6) prepared in the presence of EP with [EP]/[MAA] = 0.6. Note that most EP molecules complexed with individual hyperbranched terpolymer chains as well as only a small amount of free EP molecules are soluble in DMF. However, small free EP molecules have nearly no contribution to the scattered light intensity. From

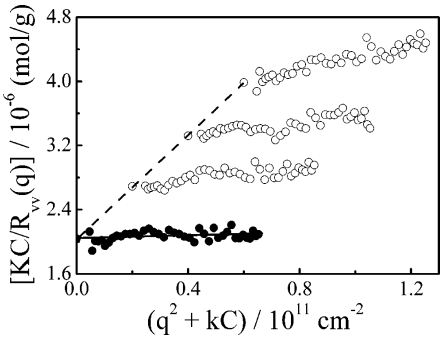

Figure 3. Zimm plot of EP-0.6 in DMF at 25 °C, where $M_{w,single}$ = 4.91 × 10^5 g/mol; $\langle R_g \rangle_{single}$ = 12.2 nm, and $A_{2,single}$ = 1.46 × 10^{-4} (mol cm^3)/g^2.

each Zimm plot, we were able to obtain M_w, $\langle R_g \rangle$, and A_2 of individual terpolymer chain ($M_{w,single}$, $\langle R_g \rangle_{single}$, and $A_{2,single}$) formed in the presence of different amounts of EP in *n*-butyl acetate.

Figure 4 shows the concentration dependence of $(R_{vv}/KC)_{\theta \to 0}$ of four different dispersions prepared with identical

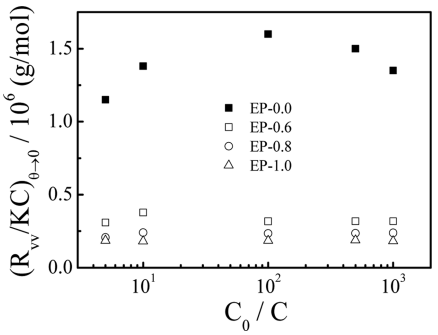

Figure 4. Concentration dependence of $(R_{vv}/KC)_{\theta \to 0}$ of four dispersions prepared with identical MAA, C_{12}-raft, and PEG_{950} contents but different contents of EP in *n*-butyl acetate, where C_0 and C represent the concentrations of original and diluted dispersions.

MAA, C_{12}-raft, and PEG_{950} contents but different EP contents in *n*-butyl acetate. Note that $(R_{vv}/KC)_{\theta \to 0}$ is the apparent weight-average molar mass ($M_{w,app}$) on the basis of eq 1. It is interesting to see that $(R_{vv}/KC)_{\theta \to 0}$ of the dispersion prepared without EP is 5−7 times higher than those prepared with EP. Also note that both $M_{w,app}$ and $M_{w,single}$ decrease as the EP content increases, indicating that the complexation between EP and MAA reduces the degree of polymerization, presumably due to the complexation induces the collapse of the chain backbone. Figure 4 also shows that $(R_{vv}/KC)_{\theta \to 0}$ of the dispersion prepared without EP slightly increases as the dispersion is diluted, i.e., a negative second virial coefficient (A_2), revealing that *n*-butyl acetate is a poor solvent for the terpolymer without EP molecules added.

Figure 5 shows that after the 1000 times dilution there exists only one narrowly distributed peak in the range of 10−20 nm in the hydrodynamic radius distribution ($f(R_h)$), showing that there is no large interchain aggregates. It is worth noting that the particle in the dispersion prepared without EP is larger (larger average hydrodynamic radius ($\langle R_h \rangle$) and $\langle R_g \rangle$) than its counterparts prepared in the presence of EP, also reflected in its slightly milky appearance, as shown in Figure 2. The ratio $\langle R_g \rangle / \langle R_h \rangle$ of these dispersions after the 1000 times dilution in *n*-butyl acetate is in the range 1.1−1.4, a typical value for hyperbranched chain conformation.[40]

The LLS results are summarized in Table 1, where all the parameters were obtained after the 1000 times dilution in *n*-butyl acetate so that there is no need to consider the concentration correction in eq 1. A combination of static LLS results in *n*-butyl acetate and DMF leads to the apparent

DOI: 10.1021/acs.macromol.5b01637
Macromolecules 2015, 48, 7327−7334

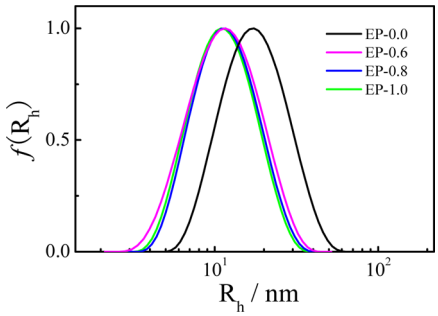

Figure 5. Intensity-weighted hydrodynamic radius distributions ($f(R_h)$) of dispersions prepared with different amounts of EP after 1000 times dilution in *n*-butyl acetate at 25 °C, where $\theta = 30°$.

aggregation number (N_{agg}); namely, $N_{agg} = M_{w,app}/M_{w,single}$. We found that $N_{agg} \sim 1$ even after a 1000 times dilution in *n*-butyl acetate, showing that the hyperbranched chains exist as unimolecular micelles in *n*-butyl acetate; namely, hydrophobic EP molecules are encapsulated inside each terpolymer chain via the complexation and stabilized by short PEG chains grafted on its periphery. Therefore, such prepared dispersions have no CMC or CAC.

A combination of Figures 2−5 validates our design principle; namely, the complexation of hydrophobic EP with MAA into the hyperbranched amphiphilic terpolymer chains not only encapsulates EP and increases the solubility of EP in *n*-butyl acetate but also induces the chain collapse, reflected in a smaller chain size, which increases τ_R, so that individual unimolecular micelle-like chains become tiny glass balls and the dispersions are more stable. Some of the previous studies also showed that loading lipophilic chemicals into polymeric micelles made the dispersion more stable.[41] However, when [EP]:[MAA] = 1.0, the dispersion prepared becomes less stable after three months and a trace amount of needle-like solid (crystallized EP) appears, indicating a slow release of the encapsulated EP from unimolecular micelles, presumably those noncomplexed EP molecules.

The structure and morphology of the EP-0.6 dispersion formed in *n*-butyl acetate were further confirmed by TEM measurements. The sample was freeze-dried to avoid a possible solvent-evaporation induced structural change and preserved the morphologies of the particles in the dispersion. Figure 6 shows typical TEM images of EP-containing particles in *n*-butyl acetate. It shows that the particles are irregular spheres with sizes in the range 10−50 nm, close to our LLS results; namely, the average hydrodynamic diameter ($2\langle R_h\rangle$) is ∼22 nm. A combination of LLS and TEM results reveals that the dispersion mainly contains unimolecular micelles in *n*-butyl acetate.

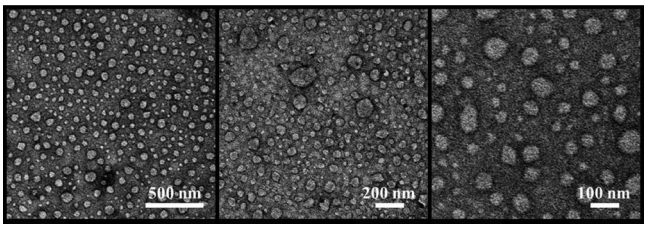

Figure 6. TEM images of EP-0.6 after its dilution in *n*-butyl acetate, where the final polymer concentration is ∼0.25 g/L.

Further, we examined the effect of the PEG_{950} content on the appearance and stability of the resultant dispersions prepared with a fixed molar ratio of [EP]:[MAA] = 0.6 and a given amount of MAA (3.03×10^{-1} M), C_{12}-raft (2.09×10^{-3} M), and EP (1.82×10^{-1} M). The solubility of PEG_{950} in *n*-butyl acetate is slightly higher than 1.5×10^{-1} g/mL. Practically, the PEG_{950} content should be kept as low as possible to reduce the cost. The experimental conditions are summarized in Table 2. Figure 7 shows only one narrowly distributed peak in the range of 10−30 nm after the 1000 times dilution in *n*-butyl acetate. $\langle R_h\rangle$ decreases, and the dispersion becomes clearer as the PEG_{950} content increases because more PEG_{950} chains are able to stabilize a larger total surface area. For a given amount of hydrophobic substances, only the formation of smaller particles can provide a larger total surface, similar to the formation of colloidal particles in a microemulsion polymerization.[42] All the LLS results of the 1000 times diluted dispersions in *n*-butyl acetate are summarized in Table 2.

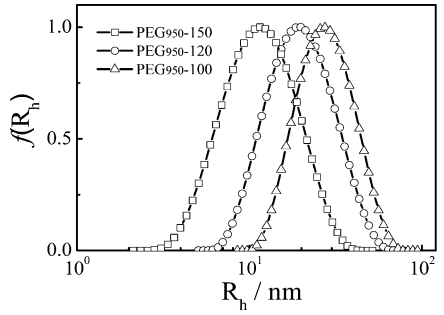

Figure 7. Intensity-weighted hydrodynamic radius distributions ($f(R_h)$) of dispersions prepared with different amounts of PEG_{950} after 1000 times dilution in *n*-butyl acetate at 25 °C, where $\theta = 30°$.

Note that the dispersions prepared are stable without any visible precipitation even after standing at room temperature for six months. It is clear that we can reduce the PEG_{950} content to 1.0×10^{-1} g/mL as long as [EP]:[MAA] ≤ 0.8. However, Table 2 shows that the particles in the dispersions contain few chains instead of unimolecular micelles when the PEG content is low, but it has no effect on their application. Also note that for PEG_{950}-150 and PEG_{950}-120 $\langle R_g\rangle/\langle R_h\rangle \sim 1.2$, a typical value for hyperbranched chains, while for PEG_{950}-100 $\langle R_g\rangle/\langle R_h\rangle \sim 0.8$, close to 0.774 for a uniform hard sphere,[40] presumably due to the interchain association that leads to a more compact and uniform structure.

Table 2. Effect of PEG_{950} Content on Appearance, Stability, and Characteristics of Resultant Dispersions Formed in One-Step Copolymerization of MAA (3.03×10^{-1} M), C_{12}-raft (2.09×10^{-3} M), and EP (1.82×10^{-1} M) in *n*-Butyl Acetate

sample	$[PEG_{950}]$ (M)	appearance	stability	$M_{w,app}$ (g/mol)	$\langle R_h\rangle$ (nm)	$\langle R_g\rangle$ (nm)	$\langle N_{agg}\rangle$
PEG_{950}-150	1.58×10^{-1}	clear	stable	3.18×10^5	11.0	13.7	0.7
PEG_{950}-120	1.26×10^{-1}	clear	stable	1.06×10^6	20.0	22.8	2.3
PEG_{950}-100	1.05×10^{-1}	slight milky	stable	3.51×10^6	27.8	22.3	8.3

DOI: 10.1021/acs.macromol.5b01637
Macromolecules 2015, 48, 7327−7334

Table 3. Effect of MAA Content on Appearance, Stability, and Characteristics of Resultant Dispersions Formed in One-Step Copolymerization of PEG_{950} (1.58×10^{-1} M), C_{12}-raft (2.09×10^{-3} M), and EP (3.03×10^{-1} M) in *n*-Butyl Acetate

sample	[EP]/[MAA]	appearance	stability	$M_{w,app}$ (g/mol)	$\langle R_h \rangle$ (nm)	$\langle R_g \rangle$ (nm)	$\langle N_{agg} \rangle$
MAA-1.00	1.0	clear	unstable	1.82×10^5	11.0	15.5	0.9
MAA-1.25	0.8	clear	stable	4.52×10^5	15.2	16.9	1.4
MAA-1.67	0.6	milky	unstable	2.07×10^6	28.0	22.0	5.0

Finally, we studied the effect of the MAA content on the appearance and stability of the resultant dispersions with a given amount of C_{12}-raft (2.09×10^{-3} M), PEG_{950} (1.58×10^{-1} M), and EP (3.03×10^{-1} M). The experimental conditions are summarized in Table 3. There is no visible precipitation or crystallization of EP in all the dispersions shortly after the copolymerization. Figure 8 shows that there exists only one

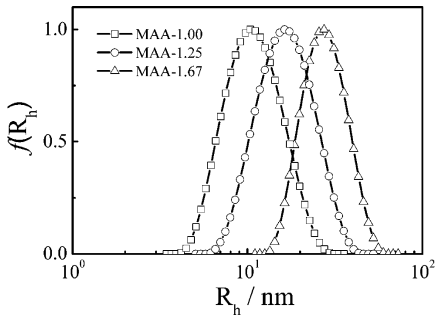

Figure 8. Intensity-weighted hydrodynamic radius distributions ($f(R_h)$) of dispersions prepared with different amounts of MAA after 1000 times dilution in *n*-butyl acetate at 25 °C, where $\theta = 30°$.

narrowly distributed peak in the range 10−30 nm after the 1000 times dilution in *n*-butyl acetate. Both $\langle R_h \rangle$ and $\langle R_g \rangle$ increase with the MAA content, also reflected in their appearances; namely, the less MAA content is the clearer the dispersion appears. This is because a given amount of PEG_{950} chains can only stabilize a certain total surface area so that more MAA would lead to a larger total surface.

The particle size increases as more MAA monomers are added since the PMAA segments are solvophobic.[42] Table 3 summarizes the LLS results of the 1000 times diluted dispersions in *n*-butyl acetate. The dispersion MAA-1.67 contains particles made of few hyperbranched terpolymer chains, revealing the existence of some interchain association. This is why $\langle R_g \rangle / \langle R_h \rangle$ decreases from 1.4 to 0.78 as the MAA content increases, namely, from a hyperbranched chain to a uniform multichain spherical aggregate.[40] In dispersion MAA-1.67, a very small amount of needle-like crystallized EP appears after several months.

The results discussed above reveal that both the monomer and EP contents affect the stability of the resultant dispersion. The optimal range of PEG_{950} is $(1.05–1.58) \times 10^{-1}$ M ($(1.0–1.5) \times 10^{-1}$ g/mL). When it is lower than 1.05×10^{-1} M, the dispersion is not stable, while 1.58×10^{-1} M is the solubility limit of PEG_{950} in *n*-butyl acetate. The content of MAA should be sufficient to complex with EP so that they are well encapsulated inside the hyperbranched chains. On the other hand, higher contents of hydrophobic MAA inevitably destabilize the dispersion. The upper limit of [EP]/[MAA] is 0.8.

The next question is whether such a formed EP dispersion stable in *n*-butyl acetate is still stable for a sufficiently long time (few hours) after its dilution in a large amount of water for the field application. Figure 9 shows a typical result of EP-0.6 after the 500 times dilution (redispersion) in water. The dispersion

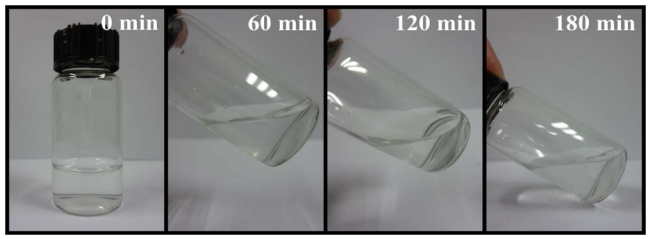

Figure 9. Photographs of time-dependent appearance and stability of EP-0.6 dispersion after 500 times dilution in water.

remains clear after 3 h, sufficiently long for its field application. Quantitatively, Figure 10 shows that there are two peaks

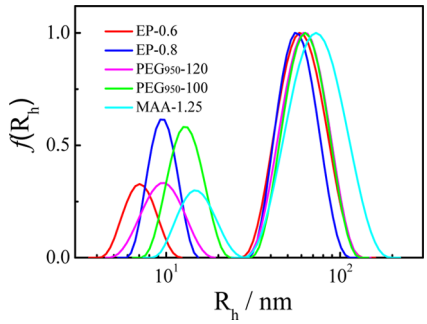

Figure 10. Intensity-weighted hydrodynamic radius distributions ($f(R_h)$) of dispersions prepared after 500 times dilution in water at 25 °C, where $\theta = 30°$.

located in the ranges of 5−15 and 60−80 nm, indicating that there exist some interchain association in water after the dilution but lead to no large aggregates and the dispersions are stable. Our novel design successfully overcomes the problem of CMC or CAC in the dilution.

Quantitatively, previous studies showed that for each given stable dispersion the average particle surface area (s) occupied per stabilizer is an important parameter and should remain a constant for a given system, namely, independent of the ratio of weight of the dispersed substance (W_d) and the stabilizing agent (W_s).[42,43] s is related to the total surface area (S), the number of the stabilizer (N_s), and the number and radius of the particle (N_p and R) as

$$s = \frac{S}{N_s} = \frac{4\pi R^2 N_p}{N_s} \quad (2)$$

where $N_p = (W_d + W_s)/(4\pi\rho R^3/3)$ and $N_s = N_A W_s / M_s$, with ρ, M_s, and N_A being the average density of the stabilized core, the stabilizer's molar mass, and Avogadro's number, respectively. We can rewrite eq 2 as

DOI: 10.1021/acs.macromol.5b01637
Macromolecules 2015, 48, 7327−7334

$$\frac{W_d + W_s}{W_s} = s\frac{N_A\rho}{3M_s}R \quad (3)$$

For a given system, ρ and M_s are constants so that the plot of $(W_d + W_s)/W_s$ versus R would be a straight line if s is a constant as expected.

Figure 11 shows such a plot. It should be noted that here we only use the values of $\langle R_h \rangle$ of those small particles in Figure 10

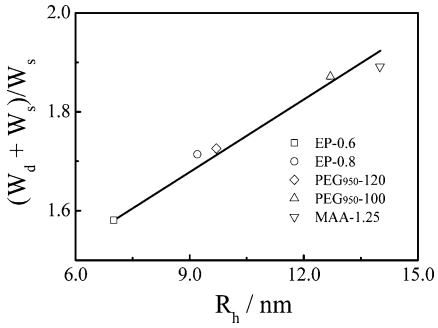

Figure 11. $(W_d + W_s)/W_s$ dependence of hydrodynamic radius of five EP/terpolymer dispersions after 500 times dilution in water, where W_d and W_s are defined in eqs 2 and 3 (see text for details).

because the distributions $(f(R_h))$ are intensity weighted. Namely, the scattered light intensity from one 100 nm particle is 10^6 times that from one 10 nm particle so that the number of the large particles in Figure 10 in each of the dispersions is fairly small even though their related peak looks large. Figure 11 clearly shows that the average surface area stabilized by each PEG chain (s) is indeed a constant. The least-squares fitting of the data points in Figure 11 leads to $(W_d + W_s)/W_s \sim 4.48 \times 10^{-2}\langle R_h \rangle$; i.e., $s \sim 1.0-0.5$ nm^2 per PEG chain on the basis of eq 3 if we assume that $\rho \sim 0.2-0.4$ g/cm^3 on our previous study of collapsed chains,[44,45] indicating that the grafting density of PEG_{950} on the periphery of each collapsed hyperbranched chain is fairly high and the PEG chains are stretched and packed on the surface or, in other words, individual particles are well protected. This explains why the dispersion is stable even after 500 times dilution in water.

To check whether and how EP is slowly released from these particles, we further measured a time-dependent release profile of EP based on the results of UV adsorption spectra after the 500 times dilution in water, as seen in Figure 12. The inset shows a typical example of EP-0.6, where the UV spectrum of the dispersion prepared without EP was used as a reference.

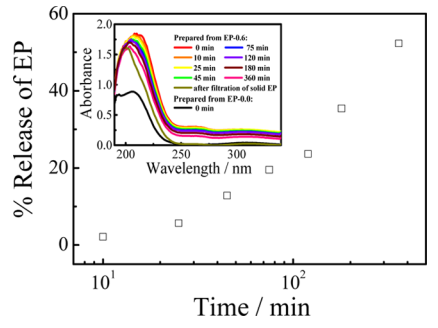

Figure 12. Time-dependent release of EP after a 500 times dilution in water, where the inset shows the UV−vis spectra of two dispersions prepared in *n*-butyl acetate (original concentration is ∼30%) after a 500 times dilution in water.

The time-dependent absorption (at 263 nm) differences between EP-0.6 and EP-0.0 clearly show that EP was slowly released. Note that after 2 h only 20% of EP was released after a 500 times dilution in water. This time is sufficiently long for the real field application. Such a slow release is what we need after the dispersion in *n*-butyl acetate is diluted into a large amount of water and spread on the leaves in the field application.

CONCLUSION

With a properly chosen composition of three starting monomers (one stabilizer: poly(ethylene glycol) methyl ether methacrylate, PEG_{950}; one complexation agent: methacrylic acid, MAA; and one vinyl-functionalized chain transfer agent, C_{12}-raft), we successfully synthesized amphiphilic hyperbranched poly(MAA-*co*-C_{12}-*g*-PEG_{950}) terpolymer in a biocompatible and nontoxic solvent, *n*-butyl acetate, via one-pot self-condensing vinyl copolymerization in a single step. Using such formed terpolymer chains, we are able to encapsulate a model hydrophobic active chemical (epoxiconazole, EP, an effective fungicide) to form micelle-like stable core−shell unimolecular colloidal particles made of individual hyperbranched terpolymer chains with a poly(MAA-*co*-C_{12})/EP core and a PEG_{950} shell. The formation of such unimolecular micelles enables us to practically avoid the instability problem in the process of diluting a dispersion made of self-assembled molecules. Our results have further confirmed an anti-intuitive stabilization mechanism on the basis of viscoelasticity. Namely, properly introducing some hydrophobic segments (C_{12}) and component (EP) promotes the stabilization of the resultant unimolecular micelle-like structures because they lead to the chain collapse inside the core and effectively make the chain relaxation time much longer than the interaction time of two colliding chains so that each approaching collapsed chain behaves like a tiny glass ball and their association is kinetically diminished. Therefore, such formed novel unimolecular micelle dispersions are stable even after 1000 times dilution in either *n*-butyl acetate or water. Our results reveal that, on average, each PEG_{950} chain grafted on the particle's periphery stabilizes a constant surface area in the range 0.5−1.0 nm^2, independent of the composition inside the core. The principle of forming such unimolecular core−shell micelle-like structures (particles) with one amphiphilic hyperbranched terpolymer chain in a one-pot process is readily applicable to encapsulate other active chemicals, including agrochemicals and drugs, if a proper set of comonomers can be designed and available. The current study has paved a novel, effective, and economic way to formulate hydrophobic chemicals into stable dispersions that have no critical micelle or association concentration so that the instability problem is avoided when they are diluted in a large amount of solvent or water for real applications.

AUTHOR INFORMATION

Corresponding Authors

*E-mail: chiwu@cuhk.edu.hk (C.W.).

*E-mail: xwang101@mail.ustc.edu.cn (X.W.).

Notes

The authors declare no competing financial interest.

ACKNOWLEDGMENTS

The financial support of the Ministry of Science and Technology of China Key Project (2012CB933800), the National Natural Scientific Foundation of China Projects

DOI: 10.1021/acs.macromol.5b01637
Macromolecules 2015, 48, 7327−7334

(51173177 and 51273091), and the Hong Kong Special Administration Region Earmarked Projects (CUHK7/CRF/12G, 2390062; CUHK4035/12P, 2130306/4053005; and CUHK4042/13P, 2130349/4053060) is gratefully acknowledged.

REFERENCES

(1) Chiou, W. L.; Riegelman, S. *J. Pharm. Sci.* **1971**, *60*, 1281.
(2) Serajuddin, A. T. M. *J. Pharm. Sci.* **1999**, *88*, 1058.
(3) Verreck, G.; Six, K.; Van den Mooter, G.; Baert, L.; Peeters, J.; Brewster, M. E. *Int. J. Pharm.* **2003**, *251*, 165.
(4) Loftsson, T.; Olafsson, J. H. *Int. J. Dermatol.* **1998**, *37*, 241.
(5) Hedges, A. R. *Chem. Rev.* **1998**, *98*, 2035.
(6) Sun, T.; Guo, Q.; Zhang, C.; Hao, J.; Xing, P.; Su, J.; Li, S.; Hao, A.; Liu, G. *Langmuir* **2012**, *28*, 8625.
(7) Szente, L.; Szejtli, J. *Adv. Drug Delivery Rev.* **1999**, *36*, 17.
(8) Humberstone, A. J.; Charman, W. N. *Adv. Drug Delivery Rev.* **1997**, *25*, 103.
(9) Constantinides, P. P.; Tustian, A.; Kessler, D. R. *Adv. Drug Delivery Rev.* **2004**, *56*, 1243.
(10) Lawrence, M. J.; Rees, G. D. *Adv. Drug Delivery Rev.* **2000**, *45*, 89.
(11) Zhang, J.; Lv, Y.; Wang, B.; Zhao, S.; Tan, M.; Lv, G.; Ma, X. *Mol. Pharmaceutics* **2015**, *12*, 695.
(12) Zhu, Z. *Mol. Pharmaceutics* **2014**, *11*, 776.
(13) Li, Y.; Wu, Z.; He, W.; Qin, C.; Yao, J.; Zhou, J.; Yin, L. *Mol. Pharmaceutics* **2015**, *12*, 1485.
(14) Aryal, S.; Prabaharan, M.; Pilla, S.; Gong, S. *Int. J. Biol. Macromol.* **2009**, *44*, 346.
(15) Kuang, H.; Wu, S.; Xie, Z.; Meng, F.; Jing, X.; Huang, Y. *Biomacromolecules* **2012**, *13*, 3004.
(16) Chen, S.; Zhang, X.-Z.; Cheng, S.-X.; Zhuo, R.-X.; Gu, Z.-W. *Biomacromolecules* **2008**, *9*, 2578.
(17) Dash, T. K.; Konkimalla, V. B. *Mol. Pharmaceutics* **2012**, *9*, 2365.
(18) Bertin, P. A.; Watson, K. J.; Nguyen, S. T. *Macromolecules* **2004**, *37*, 8364.
(19) Kabanov, A. V.; Batrakova, E. V.; Alakhov, V. Y. *J. Controlled Release* **2002**, *82*, 189.
(20) Kakizawa, Y.; Kataoka, K. *Adv. Drug Delivery Rev.* **2002**, *54*, 203.
(21) Kataoka, K.; Harada, A.; Nagasaki, Y. *Adv. Drug Delivery Rev.* **2012**, *64*, 37.
(22) Torchilin, V. P. *J. Controlled Release* **2001**, *73*, 137.
(23) Wang, F.; Bronich, T. K.; Kabanov, A. V.; Rauh, R. D.; Roovers, J. *Bioconjugate Chem.* **2005**, *16*, 397.
(24) Patri, A. K.; Majoros, I. J.; Baker, J. R., Jr. *Curr. Opin. Chem. Biol.* **2002**, *6*, 466.
(25) Liu, M.; Fréchet, J. M. J. *Pharm. Sci. Technol. Today* **1999**, *2*, 393.
(26) Gillies, E. R.; Fréchet, J. M. J. *Drug Discovery Today* **2005**, *10*, 35.
(27) Inoue, K. *Prog. Polym. Sci.* **2000**, *25*, 453.
(28) Gao, C.; Yan, D. *Prog. Polym. Sci.* **2004**, *29*, 183.
(29) Zou, J.; Zhao, Y.; Shi, W. *J. Phys. Chem. B* **2006**, *110*, 2638.
(30) Kreutzer, G.; Ternat, C.; Nguyen, T. Q.; Plummer, C. J. G.; Månson, J.-A. E.; Castelletto, V.; Hamley, I. W.; Sun, F.; Sheiko, S. S.; Herrmann, A.; Ouali, L.; Sommer, H.; Fieber, W.; Velazco, M. I.; Klok, H.-A. *Macromolecules* **2006**, *39*, 4507.
(31) Bertelsen, J. R.; De Neergaard, E.; Smedegaard-Petersen, V. *Plant Pathol.* **2001**, *50*, 190.
(32) Hutta, M.; Rybár, I.; Chalányová, M. *J. Chrom. A* **2002**, *959*, 143.
(33) Wu, C.; Li, W.; Zhu, X. X. *Macromolecules* **2004**, *37*, 4989.
(34) Hao, J.; Li, Z.; Cheng, H.; Wu, C.; Han, C. C. *Macromolecules* **2010**, *43*, 9534.
(35) Lai, J. T.; Filla, D.; Shea, R. *Macromolecules* **2002**, *35*, 6754.
(36) Chu, B. *Laser Light Scattering*; Academic Press: New York, 1974.
(37) Berne, B. J.; Pecora, R. *Dynamic Light Scattering*; Plenum Press: New York, 1976.
(38) Zimm, B. H. *J. Chem. Phys.* **1948**, *16*, 1099.
(39) Wu, C.; Xia, K. Q. *Rev. Sci. Instrum.* **1994**, *65*, 587.
(40) Li, L.; He, C.; He, W.; Wu, C. *Macromolecules* **2011**, *44*, 8195.
(41) Kim, S.; Shi, Y.; Kim, J. Y.; Park, K.; Cheng, J.-X. *Expert Opin. Drug Delivery* **2010**, *7*, 49.
(42) Wu, C.; Akashi, M.; Chen, M.-Q. *Macromolecules* **1997**, *30*, 2187.
(43) Zhang, G.; Niu, A.; Peng, S.; Jiang, M.; Tu, Y.; Li, M.; Wu, C. *Acc. Chem. Res.* **2001**, *34*, 249.
(44) Wu, C.; Zhou, S. *Macromolecules* **1995**, *28*, 8381.
(45) Wang, X.; Qiu, X.; Wu, C. *Macromolecules* **1998**, *31*, 2972.

DOI: 10.1021/acs.macromol.5b01637
Macromolecules 2015, 48, 7327−7334